Structure of Clusters in Methanol-Water Binary Solutions Studied by Mass Spectrometry and X-ray Diffraction

Toshiyuki Takamuku, Toshio Yamaguchi[a], Masaki Asato[b], Masaki Matsumoto[b], and Nobuyuki Nishi[c]

Department of Chemistry, Faculty of Science and Engineering, Saga University, Honjo-machi, Saga 840-8502, Japan

[a] Department of Chemistry, Faculty of Science, Fukuoka University, Nanakuma, Jonan-ku, Fukuoka 814-0180, Japan

[b] Department of Chemistry, Faculty of Science, Kyushu University, Hakozaki, Higashi-ku, Fukuoka 812-8581, Japan

[c] Institute for Molecular Science, Myodaiji, Okazaki 444-8585, Japan

Reprint requests to Prof. T. Y.; Fax: +81-92-865-6030; E-mail: yamaguch@sunsp1.sc.fukuoka-u.ac.jp

Z. Naturforsch. **55 a,** 513–525 (2000); received February 11, 2000

The structure of clusters in methanol-water solutions in its dependence on the methanol mole fraction x_M has been investigated by mass spectrometry on clusters isolated from submicron droplets by adiabatic expansion in vacuum and by X-ray diffraction on the bulk binary solutions. The mass spectra have shown that the average hydration number, $\langle n_m \rangle$, of m-mer methanol clusters decreases with increasing x_M, accompanied by two inflection points at $x_M = \sim 0.3$ and ~ 0.7. The X-ray diffraction data have revealed a similar change in the number of hydrogen bonds per water and/or methanol oxygen atom at ~ 2.8 Å. On the basis of both results, most likely models of clusters formed in the binary solutions are proposed: at $0 < x_M < 0.3$ the tetrahedral-like water cluster is the main species, at $0.3 < x_M < 0.7$ chain clusters of methanol molecules gradually evolve with increasing methanol content, and finally, at $x_M > 0.7$ chain clusters of methanol molecules become predominant. The present results are compared with clusters previously found in ethanol-water binary solutions and discussed in relation to anomalies of the heat of mixing of methanol-water binary solutions.

Key words: Methanol-water Binary Solutions; Mass Spectrometry; X-ray Diffraction; Clusters; Hydrogen Bonds.

1. Introduction

Solutions of alcohol and water are often used in chemical reactions, solvent extraction, high-performance liquid chromatography, etc. since their properties can be varied for individual use by changing their composition. Franks and Ives [1] reviewed physicochemical properties such as the enthalpy and entropy of mixing, and the partial molar volume for various alcohol-water mixtures. In these studies many authors have pointed out anomalies in the partial molar volume [2], ^{1}H-NMR chemical shift [3], dielectric relaxation [4 - 6], aggregation behavior of chlorophyll [7], etc., and discussed their possible origin in terms of hydrogen bonding and hydrophobic interaction. Thus, structural investigations of methanol-water mixtures are essential for understanding their unique properties.

Various structural investigations have so far been made on neat methanol by X-ray [8 - 12] and neutron [13 - 18] diffraction and molecular dynamics simulation [19, 20]. Most of the authors reached the conclusion that methanol molecules form chain clusters by hydrogen bonds. The structure of methanol-water mixtures has been investigated mostly by computer simulations [21 - 29]. Pálinkás and Bakó [27] made a molecular dynamics simulation on methanol, water, and their mixtures at methanol mole fractions x_M = 0.1, 0.25 and 0.9, and estimated excess properties such as the potential energy and heat capacity of the mixtures. They found that the excess potential energy of methanol-water mixtures has a minimum at

0932–0784 / 00 / 0500–0513 $ 06.00

$x_M = 0.25$, which is close to a minimum ($x_M \approx 0.3$) of the heat of mixing at 25 °C [1]. To our knowledge, so far only neutron diffraction experiments on a methanol-water mixture at $x_M = 0.1$ by using H/D substitution in methyl and water, were made [30], and it has been revealed that a definite hydration shell of water molecules exists at a distance of ~3.7 Å from the methyl carbon atom. Neither X-ray nor neutron diffraction studies have been performed on methanol-water mixtures over the whole range of methanol concentrations. We have previously made mass spectrometric and X-ray diffraction measurements on ethanol-water mixtures [31 - 33] and elucidated the composition and structure of hydrogen bonded clusters formed in these mixtures.

In the present study, both mass spectrometric and X-ray diffraction experiments have been performed on binary solutions of water and methanol over a whole range $0 < x_M < 1$ to determine the composition and structure of predominant clusters. On the basis of the present findings, together with the previous results on ethanol-water mixtures, an effect of hydrophobic interaction on cluster formation in these water-alcohol mixtures is discussed. Finally, a change in heat of mixing for methanol-water mixtures is discussed from the structural point of view.

2. Experimental

2.1. Preparation of Samples

Methanol (Wako Pure Chemicals, extra grade) was dried with molecular sieves 4A 1/16 for several days. Dried methanol was refluxed with a small amount of calcium oxide for several hours and distilled under ambient pressure. Doubly distilled water was used. The densities of the mixtures were determined at 25 °C with an electronic densimeter DMA 48 (Anton Paar K.G.).

2.2. Mass Spectrometry

A method of adiabatic expansion of liquid droplets in vacuum has been described in [34 - 37]. A flow of droplets was generated by hydrodynamic conversion of liquid from a notched small nozzle with a diameter of ~40 μm. These droplets were introduced into high vacuum chambers through two skimmers. We used two different mass spectrometers: a quadrupole mass spectrometer (Extrel 7-162-8 coupled with 311-12H) and a double focus spectrometer with electric and magnetic sectors (Kratos Analytical, Profile). The ionizer of the latter system was modified with a home-made ion repeller. The central part of this repeller is made of a 25-μm wire mesh with a 90% transmittance. The droplet beam is directed perpendicular to the repeller electrode. Clusters generated through adiabatic expansion in the ionizer region are ionized by electron impact of 40 eV and repelled into ion collecting lenses at a repelling voltage of 3400 V. The high ion energy can provide a spectrum with ion intensities proportional to the cluster distribution produced by expansion. For some preliminary experiments we used a quadrupole mass filter because of its high sensitivity. However, the intensity distribution obtained with this filter is highly dependent on the rf frequency and the voltage. In this work we used a double focusing spectrometer.

The average temperature of the methanol-water droplets was estimated from the mass spectral change of an aqueous solution of propionic acid with $x_A = 0.005$. The spectral pattern of this solution is highly temperature-dependent. Higher polymer hydrates become dominant with decreasing temperature. The temperature dependence of the spectrum of this solution was carefully examined for a reference aqueous solution of 2-butoxyethanol with $x_A = 0.05$ that shows an anomalous spectral change due to phase separation in the region between the lower critical temperature (49 °C) and the upper critical temperature (129 °C) [36, 37]. Because the adiabatic expansion of liquid droplets requires sufficient internal energy, the lower limit of the average droplet temperature was found to be 30 °C under the present nozzle conditions. In the present measurements the temperature of the liquid droplets was set at 35 °C.

2.3. X-ray Diffraction

X-ray diffraction measurements were carried out at room temperature (25 °C) on water, methanol, and their mixtures over the range $0 \leq x_M \leq 1$ at 0.1 intervals. A rapid liquid X-ray diffractometer (DIP301, MAC Science), combined with an imaging plate (IP) (Fuji Film Co.) as a two-dimensional detector, was used in all measurements. Details of the diffractometer and its performance have been described in [38, 39]. X-rays were generated at a rotary Mo anode operated at 50 kV and 200 mA, and then monochromatized by a flat graphite crystal to obtain Mo Kα radiation ($\lambda = 0.7107$ Å). A sample solution sealed

in a glass capillary of 1-mm inner diameter was exposed to X-rays for 3 h. The observed range of the scattering angle (2θ) was from 0.1 to 109 °, corresponding to a scattering vector s ($= 4\pi\lambda^{-1}\sin\theta$) of 0.02 to 14.4 Å^{-1}. X-ray intensities for an empty capillary were also measured for correction of the cell scattering.

2.4. X-ray Data Treatment

Two-dimensional X-ray intensities, $I_{\mathrm{obsd}}(x, y)$, for a sample solution and an empty capillary accumulated on IP were corrected for polarization and absorption and then integrated into one-dimensional data, $I_{\mathrm{obsd}}(\theta)$, as described in [38, 39]. The contribution of the sample solution was obtained by subtraction of the intensities for the empty capillary from those for the sample. The corrected intensities were then normalized to electron units in a stoichiometric volume containing one water and/or methanol O atom by conventional methods [40 - 42]. A structure function, $i(s)$, and a radial distribution function (RDF) for each sample were obtained by usual methods as described in [32]. These treatments of the X-ray diffraction data were carried out with program KURVLR [43].

To make a quantitative analysis on the above RDFs, two methods were employed in the present analysis; one is a peak separation procedure in r-space with Gaussian function, which was applied to a peak at ~2.8 Å due mainly to nearest-neighbor hydrogen-bonded interaction, and the other is a comparison in s space between the experimental structure function, $si(s)$, and a theoretical one based on a structural model.

In the peak separation procedure the RDF in the form of $D(r)/4\pi\rho_0$ was deconvoluted with Gaussian functions,

$$\frac{D_i^{\mathrm{calcd}}(r)}{4\pi\rho_0} = \left(\frac{A_i}{\sigma_i\sqrt{\pi/\ln 2}}\right)\exp\left[-\ln 2\left(\frac{r - r_{0i}}{\sigma_i}\right)^2\right], \quad (1)$$

where A_i is the peak area, r_{0i} the peak position, and σ_i the half-width at half-height of the peak for the i-th component of RDF. The peak area A_i corresponds to a coordination number, n, for an atom pair p-q. A comparison between observed and calculated $D(r)s$ was made by a least-squares fitting procedure of minimizing an error square sum,

$$U = \frac{1}{4\pi\rho_0}\sum_{r_{\min}}^{r_{\max}}\left\{D(r) - \sum_i D_i^{\mathrm{calcd}}(r)\right\}^2, \quad (2)$$

where A_i, r_{0i}, and σ_i were adjustable parameters in the r-range between $r_{\min}$ and $r_{\max}$ of interest.

On the other hand, a comparison between the experimental structure function and the model structure function was made between minimum and maximum s-values, $s_{\min}$ and $s_{\max}$, respectively, by a least-squares refinement procedure to search a minimum of an error square sum,

$$U = \sum_{s_{\min}}^{s_{\max}} s^2\left\{i_{\mathrm{obsd}}(s) - i_{\mathrm{calcd}}(s)\right\}^2, \quad (3)$$

The theoretical intensity, $i_{\mathrm{calcd}}(s)$, was calculated by

$$i_{\mathrm{calcd}}(s) = \sum_{\mathrm{i}}\sum_{\mathrm{j}} x_{\mathrm{i}} n_{\mathrm{ij}} f_{\mathrm{i}}(s) f_{\mathrm{j}}(s)\frac{\sin(r_{\mathrm{ij}}s)}{r_{\mathrm{ij}}s}\exp(-b_{\mathrm{ij}}s^2) - \sum_{\mathrm{i}}\sum_{\mathrm{j}} x_{\mathrm{i}}x_{\mathrm{j}} f_{\mathrm{i}}(s) f_{\mathrm{j}}(s)\frac{4\pi R_{\mathrm{j}}^3}{V} \cdot \frac{\sin(R_{\mathrm{j}}s) - R_{\mathrm{j}}s\cos(R_{\mathrm{j}}s)}{(R_{\mathrm{j}}s)^3}\exp(-B_{\mathrm{j}}s^2). \quad (4)$$

The first term of the right-hand side of (4) is related to the short-range interactions characterized by the interatomic distance r_{ij}, the temperature factor b_{ij} and the number of interactions n_{ij} for an atom pair i-j. The second term arises from the interaction between a spherical hole and the continuum electron distribution beyond the hole. R_{j} is the radius of the spherical hole around atom j, and B_{j} the softness parameter for emergence of the continuum electron distribution. The least-squares refinements on structure functions were made by program NLPLSQ [44].

3. Results and Discussion

3.1. Mass Spectrometry

Figure 1 shows typical mass spectra of clusters isolated from liquid droplets of methanol-water binary mixtures at $x_{\mathrm{M}} = 0.1$, 0.4, and 0.9. The adiabatic expansion of droplets at 35 °C under a vacuum of 1×10^{-3} Pa is a fragmentation process of liquid into clusters and free molecules. Internal vibrational and

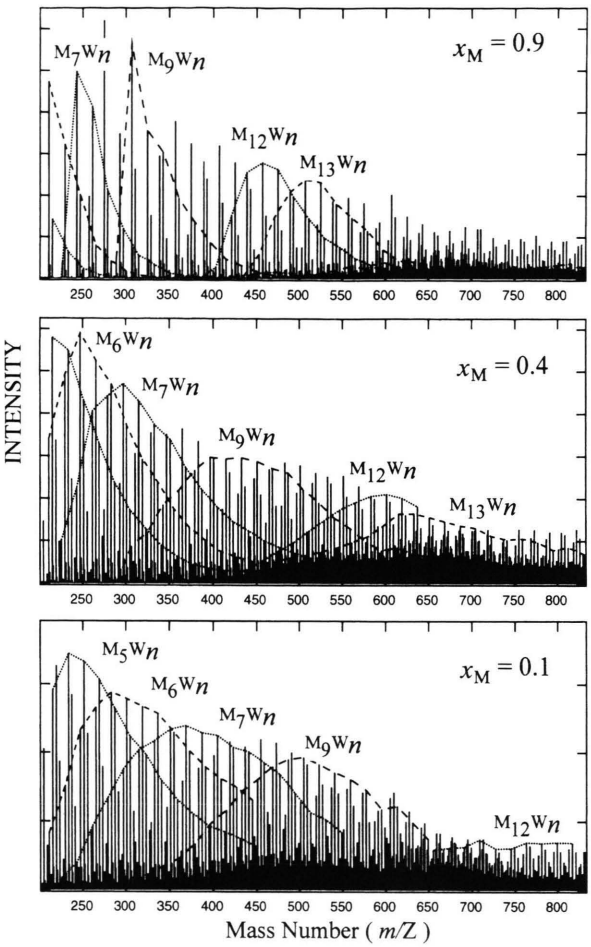

Fig. 1. Mass spectra of the clusters isolated from liquid droplets of methanol-water binary mixtures at x_M = 0.1, 0.4, and 0.9. M_mW_n stands for $H^+(CH_3OH)_m(H_2O)_n$. All the binary clusters are observed as protonated ions. This indicates that several water or methanol molecules are lost statistically from original clusters by electron impact ionization at 40 eV (see [34]). Hydration sequences of methanol m-mer hydrates are shown with broken or dotted lines. Average temperature of the droplets of the water rich solution (x_M = 0.1) was estimated to be 35±5 °C.

rotational energies are converted to translational degrees of freedom. Thus, the temperature of the clusters becomes very low. However, this cooling does not necessarily mean new intermolecular bond formation. Collisional association is a heat accumulation (or warming up) process. Collisions that could be seen by chance in the adiabatic expansion process are expected to break the clusters. Another factor causing cluster breaking is electron impact ionization. The ionization of methanol-water binary clusters can be described as dissociation processes producing free water (W) or free methanol (M) and an OH radical:

$$M_mW_n + e^- \rightarrow H^+M_mW_{n'} + OH + (n - n' - 1)W + 2e^- \quad (5)$$

or

$$\rightarrow H^+M_{m'}W_n + OH + (m - m' - 1)M + 2e^- \quad (6)$$

Hereafter, binary ions of methanol m-mer hydrates $H^+M_mW_n$ are abbreviated as M_mW_n. A previous study on ethanol-water mixtures [31, 32] demonstrated that spectral patterns do not change on varying the electron energies from 20 to 40 eV. In the present study a mass number (m/Z) range from 200 to 830 was measured to investigate clusters, since in the m/Z lower than 200, where small clusters such as monomer, dimer, trimer are concerned, ionized fragments formed by electron impact ionization at 40 eV become significant, whereas large clusters with $m/Z > 830$ are formed less often.

Cluster ions detected in mass spectra can be fragments of the liquid droplets. However, it should be born in mind that some hydrogen bonds originally weakened by intermolecular vibrational and rotational motions in the liquid can be strengthened by evaporation. Thus, the molecular composition of individual clusters might not be completely identical to that of clusters in the solution. However, it has been found that the dimerization constants of carboxylic acid clusters obtained by adiabatic expansion of mixtures of carboxylic acids and water are comparable with those determined by a calorimetric method on the corresponding bulk solutions [37]. Furthermore, our previous mass spectrometric and X-ray diffraction study on ethanol-water mixtures has shown a good coincidence of inflection points of the hydration numbers for clusters isolated from liquid droplets by mass spectrometry with those of the hydration numbers per oxygen atom of water and/or ethanol molecules obtained from X-ray diffraction on the bulk solutions [31 - 33]. Thus, it probably holds that the observed molecular composition of the clusters in the methanol-water mixtures are not very different from those of the associates in the bulk solutions, as subsequently discussed in detail.

As seen in Fig. 1, with increasing x_M, the hydration sequences of methanol m-mer hydrates become

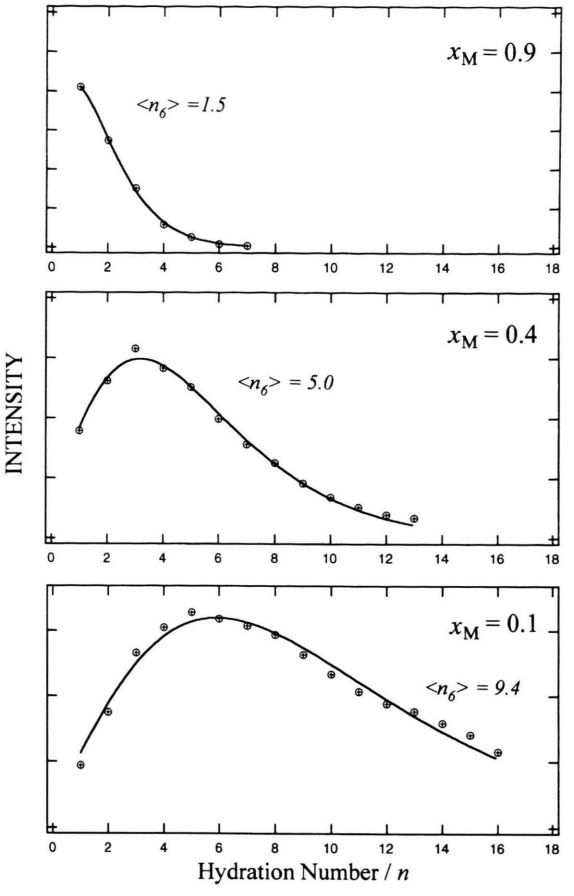

Fig. 2. Mixing ratio dependence of the intensity distributions of methanol 6-mer hydrates, M_6W_n. Average hydration numbers, $\langle n_m \rangle$, are obtained by fitting the distribution with a Γ distribution function (see (7) and (8) in text). The estimates of error in the coefficient A, a, and b in (7) are 3.8%, 12.2%, and 7.4%, respectively, for x_M = 0.9. For x_M = 0.4, those are 7.4%, 5.2%, and 4.3%, respectively: for x_M = 0.1, 12.6%, 6.2%, and 17.5%, respectively.

narrower, the intensity maxima shifting to clusters with smaller hydration numbers in the respective m-mer series. This change in the degree of hydration contrasts with that found in ethanol-water mixtures [32], where the mass spectra showed only a small change in hydration with increasing water content. The most striking feature in the mass spectra of the methanol-water mixtures is the absence of signals for non-hydrated methanol clusters M_m even at x_M = 0.9. In the ethanol-water mixtures, strong signals for non-hydrated ethanol clusters with $m < 8$ have been observed even at x_E = 0.2 in each hydration sequence.

The hydration sequences of ethanol-water clusters were approximated with the Poisson distribution function. On the other hand, it has been found that the hydration sequences for the methanol-water mixtures are expressed with a Γ distribution function, $F_m(n)$:

$$F_m(n) = A(m)n^{am-1}\exp(-bn). \quad (7)$$

Here, n corresponds to the hydration number of a methanol m-mer cluster, and a and b are constants. The extreme case with $a = m^{-1}$ corresponds to the Boltzmann-type distribution function. An average hydration number, $\langle n_m \rangle$, is given as:

$$\langle n_m \rangle = am/b. \quad (8)$$

Figure 2 shows some examples of least-squares fits with the distribution function (7) to the hydration sequences of methanol 6-mer clusters at x_M = 0.1, 0.4, and 0.9, where the average hydration numbers were 9.4, 5.0, and 1.5, respectively. As seen in the figure, the model distribution function well describes the observed intensities.

The average hydration numbers obtained for methanol 6, 8, 10, and 12-mers are shown in Fig. 3 as functions of x_M. The average hydration numbers decrease gradually with increasing mole fraction of methanol, but there appear two inflection points at x_M = ~0.3 and ~0.7. The two inflection points suggest three regimes where predominant clusters might differ in each regime, i.e. Regimes I ($x_M < 0.3$), II ($0.3 < x_M < 0.7$), and III ($0.7 < x_M < 1$). It should be noted that the inflection point at x_M = ~0.3 corresponds well to the composition where a minimum of heat of mixing at 25 °C has been observed [1].

The average hydration numbers in the three regimes can be reproduced empirically by the following equations:
In Regime I,

$$\langle n_m \rangle = 3(m-0.5)(x_W-0.3)^2+0.45(m-3.8), \quad (9)$$

in Regime II,

$$\langle n_m \rangle = m(x_W - 0.3) + 1.4(m - 3.8), \quad (10)$$

and in Regime III,

$$\langle n_m \rangle = 4.3(m - 3.8)x_W. \quad (11)$$

These equations were obtained by the curve-fitting procedures for all experimental points over the x_M

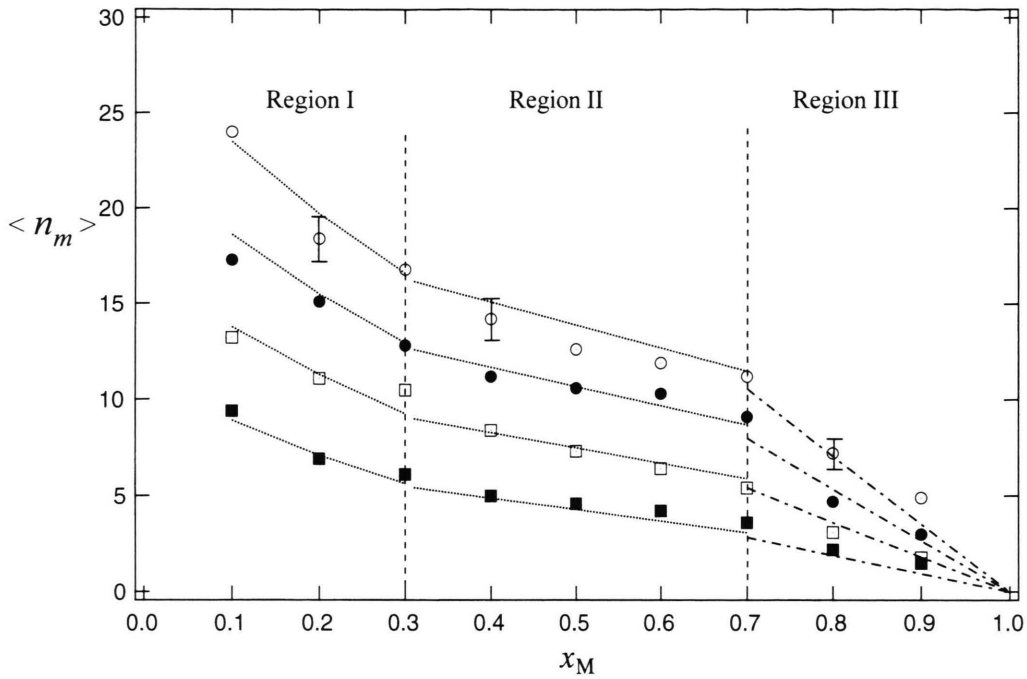

Fig. 3. Plots of average hydration numbers, $\langle n_m \rangle$, for the methanol m-mer hydrates with $m = 6$ (■), 8 (□), 10(●), and 12(○) as functions of methanol mole fractions (x_M). Dotted lines were obtained from the equations: $\langle n_m \rangle = 3(m - 0.5)(x_W - 0.3)^2 + 0.45(m - 3.8)$ for Regime I ($0 < x_M \leq 0.3$), $\langle n_m \rangle = m(x_W - 0.3) + 1.4(m - 3.8)$ for Regime II ($0.3 < x_M < 0.7$), and $\langle n_m \rangle = 4.3(m - 3.8)x_W$ for Regime III ($0.7 \leq x_M \leq 1$), where x_W is the mole fraction of water. These equations were obtained by the curve-fitting procedures for all the experimental points in the respective regions. The values of 3σ are 2.2 in Regime I, 2.3 in Regime II, and 1.7 in Regime III as indicated in the figure.

values investigated in the respective regions. In Regime I, the average hydration number of methanol m-mer unit increases quadratically with increasing water mole fraction, x_W, while it increases linearly in Regime II. Over the whole methanol composition the experimental data for methanol 12-mer were not well reproduced with these equations. This is because the individual mass signals for the methanol 12-mers were not well separated due to low signal resolution for clusters of high mass numbers. The 3σ values in the observed data for methanol 12-mer are shown in Figure 3.

Here, we point out some differences in the trend of average hydration numbers with alcohol mole fraction between the methanol-water and ethanol-water [32] mixtures. For the ethanol-water mixtures only one but very sharp inflection point has been observed at $x_E = \sim 0.2$, where the heat of mixing for ethanol-water mixtures shows a minimum at 25 °C [1]. In our previous studies [31 - 33], it has been concluded that a drastic change in cluster structure in ethanol-water mixtures occurs at $x_E = \sim 0.2$. In contrast, the average hydration numbers for m-mer methanol clusters do not change very sharply with the mole fraction of methanol, and two inflection points have been observed.

Furthermore, the hydration numbers in the individual m-mer methanol clusters are remarkably larger than those for ethanol clusters, e. g. ~9 and ~25 for the 6-mer and 12-mer methanol clusters, respectively, at $x_M = 0.1$, while less than 2 and ~8 for the 6-mer and 12-mer ethanol clusters, respectively, at $x_E = 0.1$ [32]. These findings suggest that methanol clusters can accommodate a large amount of water molecules and that the cluster structures change moderately from the tetrahedral-like structure of water to a chain-like structure of methanol with an increase in methanol concentration.

3.2. X-ray Diffraction

The s-weighted structure functions over the whole range of methanol mole fractions are shown in Figure 4. The corresponding RDFs in the $D(r) - 4\pi r^2 \rho_0$

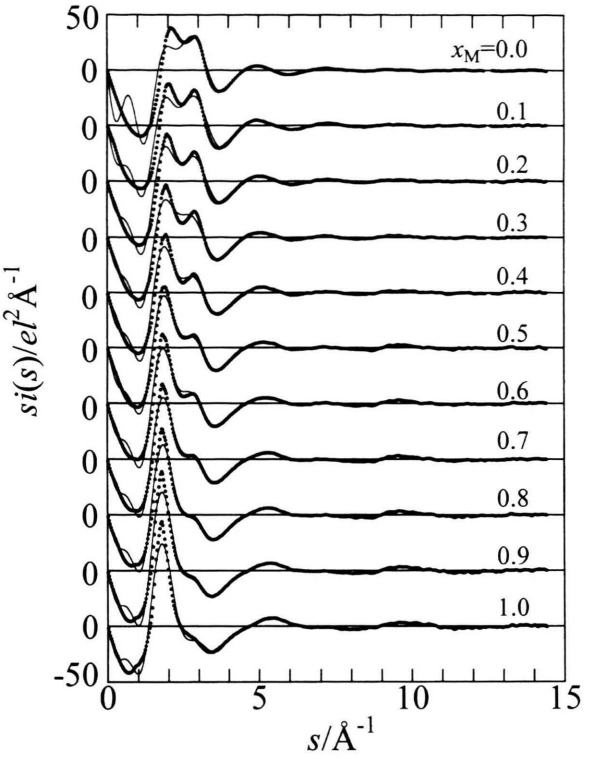

Fig. 4. Structure functions $i(s)$ multiplied by s for pure methanol and water and methanol-water mixtures at various mole fractions of methanol x_M. The dotted and solid lines are experimental and calculated ones, respectively.

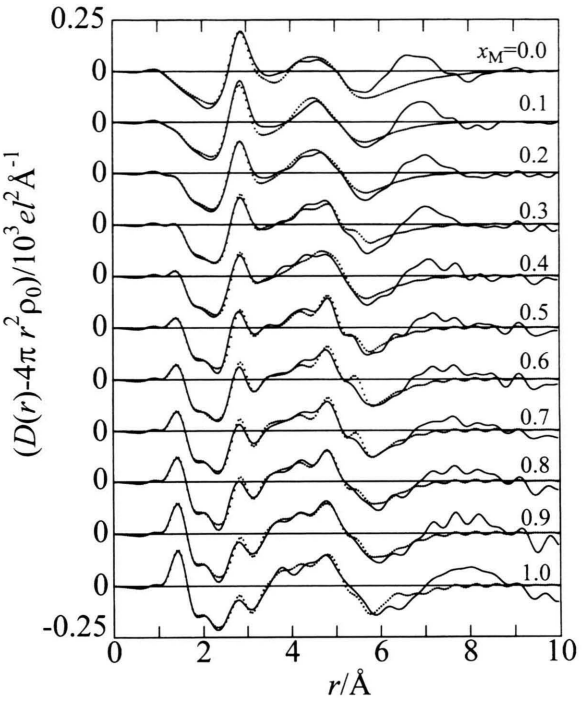

Fig. 5. Radial distribution functions in the form of $D(r) - 4\pi r^2\rho_0$ for pure methanol and water and methanol-water mixtures at various mole fractions of methanol x_M. The solid and dotted lines are experimental and calculated ones, respectively.

form are depicted in Figure 5. Corrections for periodic ripples caused by the finite termination in the Fourier transform were made up to 2.2 Å in the usual procedure [43] since the intramolecular structures of methanol [15] and water [45] have been established in the liquid phase and are not of concern in the present study. The employed interatomic distances within a methanol molecule were those previously determined by neutron diffraction measurements [15]; 0.990 Å (O-H bond), 1.085 Å (C-H), 1.435 Å (C-O), 1.77 Å (non-bonding H···H), 2.03 Å (C···H(OH) interaction) and 2.07 Å (non-bonding O···H(CH_3)). Other small periodic peaks observed in the r-range of 6 - 10 Å, as seen in the RDFs of x_M = 0.4 - 0.9, should not be assigned to any physically meaningful interactions, but to ripples due to the quality of experimental data because the long-range interactions in liquids usually give broad peaks. In the present analysis no further corrections of the ripples, e. g. data smoothing procedure, were made, however.

3.3. Total RDFs

In the RDF for neat methanol (x_M = 1.0) the intermolecular interactions are observed as a peak ~2.8 Å and broad peaks centered at ~4.5 Å and ~8 Å, consistent with the literature data [10, 11]. The peak at 2.8 Å has been assigned to O···O hydrogen bonds between methanol molecules in the literature [10, 11, 18]. The large broad peak over 3~6 Å consists of various intermolecular interactions in the first- and second-neighbors of hydrogen-bonded methanol clusters. Figure 6 shows interatomic distances expected for *trans*- and *cis*-conformations of hydrogen-bonded methanol molecules. According to the models, possible contributors to the peak are C···O (*cis* and *trans*) at ~3.4 Å, C···C (*cis*) at ~3.7 Å, C···C and O···O (*trans*) and O···O (*cis*) at ~4.5 Å, C···O (*trans*) at 4.8 Å. In liquid methanol, intermediate conformations between *trans*- and *cis*-structures would also be plausible, giving rise to the broad intermolecular peak in the RDFs. Another broad peak is observed at 6.5~10 Å, suggesting that liquid methanol

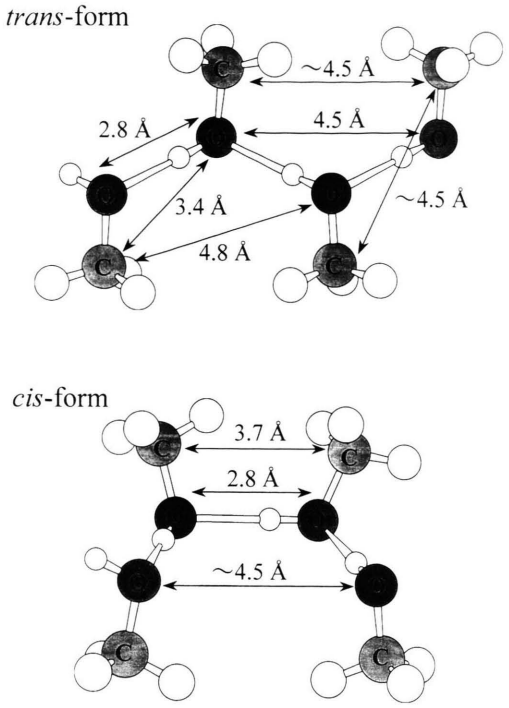

Fig. 6. Structure models of methanol chains in *trans*- and *cis*-forms.

is structured up to the fourth-neighbor as discussed by Magini *et al.* [10].

The RDF for water ($x_M = 0.0$) in Fig. 5 shows three typical peaks at 2.8, 4.5, and 7 Å, assigned to the first-, second-, and third-neighboring water molecules from a given molecule, respectively, within the tetrahedral-like ordering of water molecules in the bulk [46, 47].

When the mole fraction of methanol increases from $x_M = 0$ to 1, there appear characteristic changes in the RDFs; (i) a gradual decrease in the 2.8-Å peak due to the hydrogen bonding, (ii) a change in peak shape characteristic for water at ~4.5 Å to that for methanol over 3 ~ 6 Å, (iii) broadening and a shift to the longer distance of the third-neighbor peak over 6 ~ 9 Å. These findings demonstrate that with increasing methanol concentration the tetrahedral-like structure of water is gradually ruptured, followed by evolution of the chain-like structure of methanol. It should be stressed that the overall feature of RDF does not change so drastically as has been observed for ethanol-water mixtures [32]. This result is in good agreement with that obtained by mass spectrometry in the previous section.

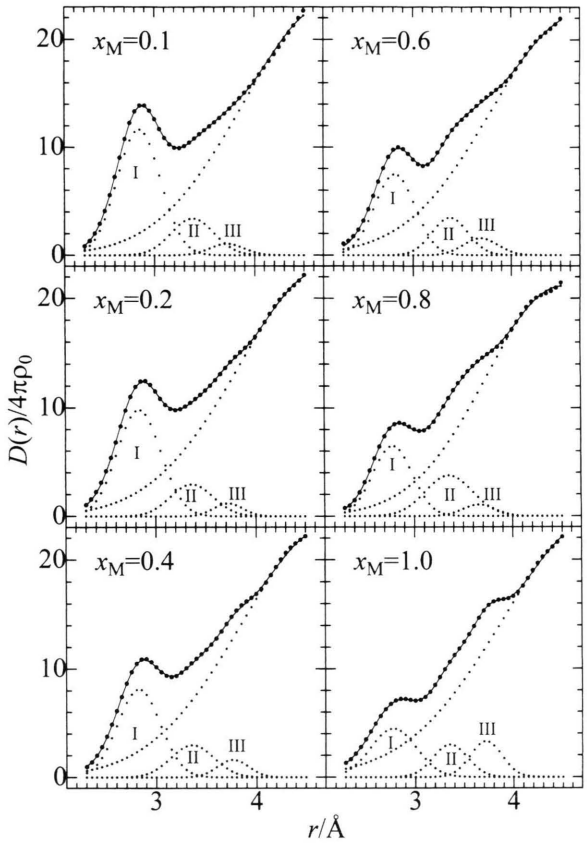

Fig. 7. Examples of the peak analysis of radial distribution functions (RDFs). The experimental values are given by filled circles, each component deconvoluted by dots, and the total theoretical values by solid lines.

3.4. Peak Separation Procedure

The details of hydrogen bonding in the methanol-water mixtures were quantitatively analyzed by a peak fitting procedure with (1) and (2) applied to the RDF in the form of $D(r)/4\pi\rho_0$ over $2.3 \leq r/\text{Å} \leq 4.5$. In the peak separation procedure, all possible interactions contributing to this region discussed in the previous section were taken into account. They were (i) predominant O-O hydrogen bonds (~2.8 Å) between water and water, water and methanol, and methanol and methanol molecules, (ii) non-hydrogen bonded interactions (~3.4 Å) related to interstitial water molecules [38, 46, 47], and (iii) interactions at ~3.7 Å of non-bonding C-O between hydrogen-bonded methanol molecules, non-bonding C···C between the hydrogen-bonded methanol molecules in a *cis*-form, and C···O due to hydrophobic hydration

Table 1. Optimized parameter values of O-O hydrogen bonds from a peak separation procedure applied to RDFs for water, methanol, and their mixtures at various methanol mole fractions. The intermolecular distance r (Å), the half-width at half-height of the peak σ (Å), the coordination number n. The values in parentheses are estimated standard deviations of the last figure.

	Hydrogen bond O···O		
x_M	r	σ	n
0.0	2.87(1)	0.28(1)	3.4(1)
0.1	2.84(1)	0.25(1)	3.1(1)
0.2	2.83(1)	0.26(1)	2.8(1)
0.3	2.84(1)	0.25(1)	2.7(1)
0.4	2.82(1)	0.25(1)	2.6(1)
0.5	2.81(1)	0.24(1)	2.6(1)
0.6	2.82(1)	0.24(1)	2.5(1)
0.7	2.79(1)	0.24(1)	2.5(1)
0.8	2.78(1)	0.23(1)	2.3(1)
0.9	2.77(1)	0.24(1)	2.0(1)
1.0	2.76(1)	0.25(1)	1.9(1)

around the methyl groups [30]. Further long-range interactions were treated as background. In the peak separation procedure, values of parameters A, r_0, and σ in (1) for background and r_{max} do affect parameter values of peaks concerned. Thus, we first made some preliminary fits to the RDFs by varying the r_{max} value from 4.5 to 4.8 Å. When r_{max} was set at distances longer than 4.5 Å, one Gaussian function could not satisfactorily reproduce the observed data over 4.0 to 4.8 Å. Thus, the r_{max} value was fixed at 4.5 Å in the present analysis. Final parameter values of the background were fixed to those that best reproduced the experimental data over 4.0 to 4.5 Å in the individual RDFs. The parameters of the other peaks were allowed to vary independently and converged uniquely. Final results of the fits are shown in Fig. 7, where the sum of the four components reproduced the observed data well.

The optimized parameter values of hydrogen bonds (peak I) for water, methanol and methanol-water mixtures are summarized in Table 1, and the number of hydrogen bonds is plotted in Fig. 8 as a function of x_M. Uncertainties in parameters r, σ, and n were estimated to be ±0.01 Å, ±0.01 Å, and ±0.1, respectively. The number of hydrogen bonds (n) in the mixtures was obtained by first scaling the A value of peak I for pure water to the hydration number (n) of water in the literature [46, 47] and then applying the scaling factor obtained to the A values of peak I for the methanol-water mixtures. The number of hydrogen bonds for pure methanol determined in this procedure was 1.87±0.04, comparable with that (1.77±0.07) recently determined for pure deuterated methanol by neutron diffraction [18]. With increasing mole fraction of methanol, the number for hydrogen bonds gradually decreases; two inflection points are observed at x_M = ~0.3 and ~0.7, as seen in Fig. 3 for the mass spectra.

The distance (2.76±0.01) Å of O···O hydrogen bonds in pure methanol agrees well with that (2.75±0.02) Å determined from a neutron diffraction experiment [18]. Narten and Habenschuss [11] estimated the distance of O···O hydrogen bonds to be (2.798±0.006) Å for methanol by X-ray diffraction. The distance (2.87±0.01) Å of O···O hydrogen bonds in pure water is comparable with a literature value (2.85 Å) previously determined by Narten and Levy [46, 47]. When the mole fraction of methanol increases from 0 to 1, the distance of O···O hydrogen bonds gradually shortened from (2.87±0.01) Å at x_M = 0 to (2.76±0.01) Å at x_M = 1.

3.5. Least-squares Refinements for Structure Functions

In order to analyze quantitatively molecular conformations between methanol-methanol, methanol-water, and water-water interactions, and also to confirm the results of the peak analysis in r-space in the previous section, a model fitting procedure using (3) and (4) was applied to the structure functions in s-space in Figure 4.

First, plausible model parameters were searched by a trial-and-error method in r-space over 0 to 6 Å. In the models the intramolecular interactions within methanol [15] and water [45] molecules were taken into account. The long-range interactions beyond 6 Å were treated as continuum electron distribution [43] since the RDFs are too broad to make unique assignments of interactions. The interactions appearing in the intermediate r-range between 2 and 6 Å were considered by building up plausible models. For pure methanol a conformation of a hydrogen-bonded chain could not be uniquely determined from X-ray diffraction because of no significant difference between the X-ray scattering factors of C and O atoms and the flexibility of hydrogen-bonded methanol chains due to small methyl-methyl hydrophobic interaction. Thus, the two chain structures of *trans*- and *cis*-forms in Fig. 6 were assumed with varying fractions of both forms. For pure water, the first- and second-neigh-

Table 2. Optimized parameter values of the interactions in water, methanol and their mixtures at various methanol mole fractions by a least-squares refinement on structure functions over the s-range $0.1 \leq s/\text{Å}^{-1} \leq 14.4$. The interatomic distance r (Å), the temperature factor b (Å^2), the number of interactions n per molecule. The values in parentheses are estimated standard deviations of the last figure. The parameters without standard deviations were not allowed to vary in the calculations.

Interaction	Parameter	x_M = 0.0	0.1	0.2	0.3	0.4	0.5	0.6	0.7	0.8	0.9	1.0
Linear hydrogen bond of water-water, methanol-water, and methanol-methanol												
O···O	r	2.826(2)	2.817(1)	2.816(1)	2.825(1)	2.822(2)	2.829(2)	2.822(2)	2.811(2)	2.812(2)	2.803(2)	2.771(4)
	10^3b	17	15	15	12	9	8	8	8	8	8	8
	n	3.43(3)	3.24(2)	3.03(2)	2.91(2)	2.64(3)	2.53(3)	2.45(2)	2.36(2)	2.11(2)	1.90(2)	1.73(3)
Interstitial water molecules												
O···O	r	3.35	3.35	3.35	3.35	3.35	3.35					
	10^3b	15	30	30	30	30	30					
	n	1.0	1.0	0.8	0.8	0.5	0.5					
1st neighbor of methanol-water and methanol-methanol												
C···O	r		3.40	3.40	3.40	3.40	3.40	3.40	3.40	3.38	3.38	3.36
	10^3b		25	25	25	25	25	25	25	25	25	25
	n		3.0	3.0	3.0	3.0	3.0	3.0	2.8	2.5	2.2	2.0
1st neighbor of methanol-methanol in *cis*-form												
C···C	r						3.70	3.70	3.70	3.70	3.70	3.70
	10^3b						30	30	30	30	30	30
	n						0.8	1.3	1.3	1.3	1.5	2.0
2nd neighbor of water-water												
O···O	r	4.00	4.00	4.00	4.00							
	10^3b	90	50	40	40							
	n	3.0	2.6	2.6	2.4							
2nd neighbor of water-water and methanol-water												
O···O	r	4.50	4.50	4.50	4.50	4.50	4.50	4.50	4.50	4.50	4.50	4.50
	10^3b	90	40	40	40	40	40	40	40	40	40	40
	n	3.0	1.5	1.5	1.5	1.5	1.5	1.5	1.5	1.5	1.5	1.5
2nd neighbor of methanol-methanol in *trans*-form												
C···C	r					4.50	4.50	4.50	4.50	4.50	4.50	4.50
	10^3b					40	40	40	40	40	40	40
	n					0.3	0.3	0.8	0.8	0.8	1.3	1.5

bors of water molecules in the tetrahedral-like structure were considered, together with interstitial water molecules at ~3.4 Å. Models for the methanol-water mixtures were built up in r-space in a trial-and-error manner by modifying both the number of interatomic interactions and the temperature factor within the chain structure of neat methanol and the tetrahedral-like structure of water depending on the composition of the mixtures. Next, by using the structural models obtained in r-space, the least-squares fitting procedure with (3) and (4) was applied to the structure functions of methanol, water, and their mixtures over the s-range from 0.1 to 14.4 Å^{-1}.

The important optimized values of structure parameters are listed in Table 2. In Figs. 4 and 5, the theoretical $si(s)$ and RDFs, calculated by using all the optimized values, reproduced the observed values well, except for the range of $s <$ ~3.5 Å^{-1} and $r \geq$ ~6 Å for which the long-range interactions, not taken into account in the present analysis, are responsible. The distance (2.771±0.004) Å of O···O hydrogen bonds for pure methanol is in good agreement with those (2.76±0.01) and (2.75±0.02) Å determined by the peak separation procedure and a neutron diffraction experiment [18], respectively. The distance (2.826±0.002) Å of O···O hydrogen bonds for pure water is slightly shorter than (2.87±0.01) Å from the peak separation procedure. This may arise from uncertainties inherent in both methods. However, the shortening of hydrogen bond O···O distances with

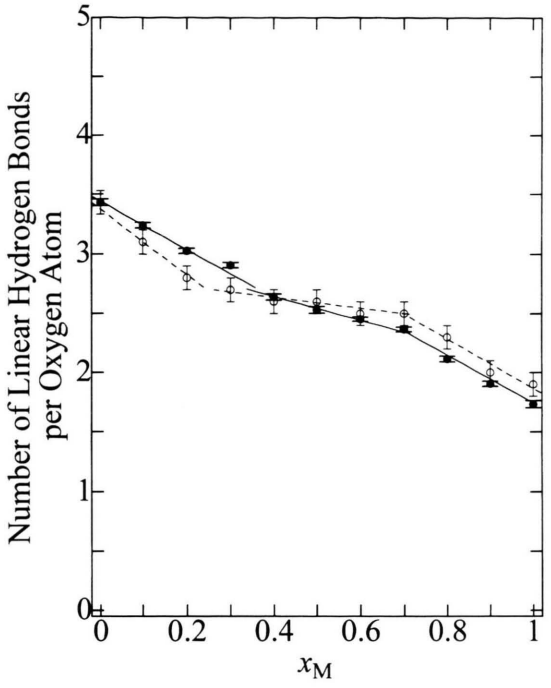

Fig. 8. Methanol mole fraction dependence of the coordination number per oxygen atom within both methanol and water molecules. The values determined by a peak separation procedure are given by opened circles, those from a least-squares refinements by filled circles, together with the standard deviation of σ values as error bars.

increasing methanol concentration has been clearly observed in both results. The number (3.43±0.03) of the hydrogen bond for pure water agrees well with a value previously determined [46, 47].

In the methanol-water mixtures, the number of hydrogen bonds gradually decreases down to 1.73±0.03 for pure methanol with an increase in methanol concentration. In Fig. 8 the numbers of hydrogen bonds at ~2.8 Å from the model fits in s-space are plotted against the mole fraction of methanol, and are in satisfactory agreement with those by the peak separation procedure. However, systematic differences in n-values, which are beyond estimated uncertainties, are obtained by both methods. These discrepancies may originate from ambiguities not completely solved in the present analyses, such as correlation among parameters employed, etc. Nevertheless, we would like to emphasize that both results have shown two inflection points at x_M = ~0.3 and ~0.7, as reported in the literature [1, 6, 7]. Therefore, together with the result from the mass spectrometry, the present X-ray diffraction data strongly suggest that predominant cluster structures in methanol-water mixtures change at these compositions.

Here, it should be mentioned that the present model given in Table 2 should be regarded as one of the models to reproduce the experimental data of the methanol-water mixtures. Neutron diffraction with H/D substitution in methanol and water mixtures would give more definite models of the mixtures.

All of the present results indicate that clusters are present in the methanol-water mixtures: as seen in Table 2, in the range of $0 \leq x_M < 0.3$ the first and second neighbor H_2O-H_2O interactions as well as those for the interstitial water molecules, characteristic for bulk water, remain the same to a large extent, and that the first and second neighbor C-C interactions for methanol do not appear; thus, the tetrahedral-like structure of water is predominant in this concentration range. The average hydration numbers, $\langle n_m \rangle$, of individual m-mer methanol clusters, M_mW_n, estimated from the mass spectrometry have shown that the methanol clusters are surrounded by about twice as many water molecules than methanol (Fig. 3); it is thus likely that methanol molecules can be embedded into the hydrogen-bonded network of water.

In the range of $0.3 < x_M < 0.7$, the numbers of the second-neighbor and interstitial water molecules for the tetrahedral-like water structure decrease substantially or disappear when $x_M > 0.4$. On the other hand, the numbers of the first- and second-neighbor C···C interactions in methanol chains gradually increase with increasing mole fraction of methanol. These data suggest that the chain-like clusters of methanol are gradually evolved in the mixtures in the range of $x_M > \sim 0.3$. It should be noted that such a structural transition is not so sharp as that observed for ethanol-water mixtures. With further increase in x_M from 0.7 to 1 the average hydration numbers of individual methanol clusters rapidly decrease, and the numbers of the first- and second-neighbor C···C interactions in the methanol chains further increase. It is thus concluded that the chain clusters of methanol are predominant in the mixtures when x_M exceeds 0.7.

3.6. Heat of Mixing

The heat of mixing for methanol-water mixtures at 25 °C is negative over the whole range of x_M [1]. A minimum of ΔH = ~850 J mol^{-1} appears at x_M = ~0.3 [1]. In addition, there is another small inflection

point at $x_M = \sim 0.7$. These two inflection points in heat of mixing corresponds remarkably well to those for both the average hydration number for methanol clusters by mass spectrometry (Fig. 3) and the number of hydrogen bonds by X-ray diffraction (Fig. 8). It is thus most probable that the heat of mixing for methanol-water reflects the structure of clusters formed.

The negative heat of mixing probably arises from stabilization of methanol molecules in the tetrahedral structure of water by more strengthened hydrogen bonds among methanol and/or water molecules than in neat methanol. Pálinkás and Bakó [27] reproduced stabilization of methanol molecules in methanol-water mixtures from excess potential energies by a molecular dynamics simulation. In the range of $0 < x_M < 0.3$, methanol molecules will be stabilized in the water structure without considerable disruption of the water structure and are most stabilized at $x_M = \sim 0.3$, where a minimum of the heat of mixing is observed. Over the range of $0.3 < x_M < 0.7$, the inherent water structure is gradually broken and/or weakened by formation of methanol chains; thus, the heat of mixing gradually becomes less negative with increasing x_M. At $x_M > 0.7$, the chain clusters of methanol become predominant, and the hydrogen-bonded network of water forms little; the stability of the methanol clusters will be lowered, resulting in a less negative heat of mixing.

For ethanol-water mixtures the heat of mixing at 25 °C is also negative over the whole mole fraction range with a minimum of $\Delta H = \sim 730$ J mol^{-1} at $x_E = \sim 0.2$ [1], and again suggests stabilization of ethanol molecules in ethanol-water mixtures at $x_E < \sim 0.2$. However, the heat of mixing for methanol-water mixtures is more negative and more gradually changes against x_M over most of mole fractions than that for the ethanol-water mixtures. Hence, it is likely that the smaller hydrophobic methyl group of a methanol molecule is more stabilized in aqueous mixtures than the ethyl group of an ethanol molecule, and that the larger hydrophobic groups of ethanol molecules more quickly disturb the tetrahedral structure of water with increasing mole fraction of ethanol, sandwich structure clusters being formed by hydrophobic interaction at $x_E = \sim 0.2$ [31 - 33].

4. Conclusion

Combined mass spectra and X-ray diffraction data have revealed a change in average clusters formed in methanol-water mixtures. At low methanol mole fractions ($x_M < 0.3$) the mixture is governed by the tetrahedral-like water clusters, but at $0.3 < x_M < 0.7$ the inherent water clusters are gradually replaced by methanol clusters of chain structure without significant disruption of the water structure, and finally at high alcohol mole fractions ($x_M > 0.7$) the chain structure of methanol becomes predominant in the solutions. A comparison of the present results on the methanol-water mixtures with those of ethanol-water mixtures shows that the tetrahedral-like water structure is broken down at a lower mole fraction (0.2) and more sharply in the ethanol-water mixtures than in the methanol-water mixtures due to the large hydrophobic effect of ethanol. The behavior of the heat of mixing with alcohol concentration in the methanol-water mixtures is consistent with that of the average clusters formed in the mixtures, and thus anomalies in the physico-chemical data of alcohol-water probably originate from clusters formed in the mixtures.

Acknowledgements

This work was supported in part by a Joint Studies Program (1997 - 1998) of the Institute for Molecular Science, by a Grant-in-Aid for Encouragement of Young Scientists (No. 09740444) (T T.), and a Grant-in-Aid B (No. 09440207) (T. Y.) from the Japanese Ministry of Education, Science, Sports and Culture.

[1] F. Franks and D. J. G. Ives, Q. Rev. Chem. Soc. **20**, 1 (1966).
[2] K. Nakanishi, Bull. Chem. Soc. Japan **33**, 793 (1960).
[3] A. Coccia, P. L. Inodovia, F. Podo, and V. Viti, Chem. Phys. **7**, 30 (1975).
[4] S. Mashimo, S. Kuwabara, S. Yagihara, and K. Higasi, J. Chem. Phys. **90**, 3292 (1989).
[5] N. Asaka, N. Shinyashiki, T. Umehara, and S. Mashimo, J. Chem. Phys. **93**, 8273 (1990).
[6] S. Mashimo, T. Umehara, and H. Redlin, J. Chem. Phys. **95**, 6257 (1991).
[7] T. Oba, M. Mimuro, Z.-Y. Wang, T. Nozawa, S.Yoshida, and T. Watanabe, J. Phys. Chem. B **101**, 3261 (1997).
[8] G. G. Harvey, J. Chem. Phys. **6**, 111 (1938).
[9] D. L. Wertz and R. K. Kruh, J. Chem. Phys. **47**, 388 (1967).
[10] M. Magini, G. Paschina, and G. Piccaluga, J. Chem. Phys. **77**, 2051 (1982).

[11] A. H. Narten and A. Habenschuss, J. Chem. Phys. **80**, 3387 (1984).
[12] S. Sarkar and R. N. Joarder, J. Chem. Phys. **99**, 2032 (1993).
[13] D. G. Montague, J. C. Dore, and S. Cummings, Mol. Phys. **53**, 1049 (1984).
[14] D. G. Montague and J. C. Dore, Mol. Phys. **57**, 1035 (1986).
[15] Y. Tanaka, N. Ohtomo, and K. Arakawa, Bull. Chem. Soc. Japan **57**, 644 (1984).
[16] Y. Tanaka, N. Ohtomo, and K. Arakawa, Bull. Chem. Soc. Japan **58**, 270 (1985).
[17] F. J. Bermejo, F. J. Mompeán, J. Santoro, D. C. Steytler, and J. C. Dore, J. Mol. Liquids **33**, 183 (1987).
[18] T. Yamaguchi, K. Hidaka, and A. K. Soper, Mol. Phys. **26**, 1159 (1999).
[19] G. Pálinkás, E. Hawlicka, and K. Heinzinger, J. Phys. Chem. **91**, 4334 (1987).
[20] G. Pálinkás, Y. Tamura, E. Spohr, and K. Heinzinger, Z. Naturforsch. **43a**, 43 (1988).
[21] G. Bolis, G. Corongiu, and E. Clementi, Chem. Phys. Lett. **86**, 299 (1981).
[22] W. L. Jorgensen and J. D. Madura, J. Amer. Chem. Soc. **105**, 1407 (1983).
[23] S. Okazaki, H. Touhara, and K. Nakanishi, J. Chem. Phys. **81**, 890 (1984).
[24] P. F. W. Stouten and J. Kroon, Mol. Simul. **5**, 175 (1990).
[25] M. Ferrario, M. Haughney, I. R. McDonald, and M. L. Klein, J. Chem. Phys. **93**, 5156 (1990).
[26] G. Pálinkás, I. Bakó, K. Heinzinger, and P. Bopp, Mol. Phys. **73**, 897 (1991).
[27] G. Pálinkás and I. Bakó, Z. Naturforsch. **46a**, 95 (1991).
[28] H. Tanaka, J. Walsh, and K. E. Gubbins, Mol. Phys. **76**, 1221 (1992).
[29] H. Tanaka and K. E. Gubbins, J. Chem. Phys. **97**, 2626 (1992).
[30] A. K. Soper and J. L. Finney, Phys. Rev. Lett. **71**, 4346 (1993).
[31] N. Nishi, S. Takahashi, M. Matsumoto, A. Tanaka, K. Muraya, T. Takamuku, and T. Yamaguchi, J. Phys. Chem. **99**, 462 (1995).
[32] M. Matsumoto, N. Nishi, T. Furusawa, M. Saita, T. Takamuku, M. Yamagami, and T. Yamaguchi, Bull. Chem. Soc. Japan **68**, 1775 (1995).
[33] N. Nishi, M. Matsumoto, S. Takahashi, T. Takamuku, M. Yamagami, and T. Yamaguchi, Structures and Dynamics of Clusters; T. Kondow, K. Kaya, and A. Terasaki, ed., Universal Academy Press, Inc. and Yamada Science Foundation, 1996, pp.113-120.
[34] N. Nishi, K. Koga, C. Ohshima, K. Yamamoto, U. Nagashima, and K. Nagami, J. Amer. Chem. Soc. **110**, 5246 (1988).
[35] N. Nishi, Z. Phys. D-Atoms, Mol. Clusters **15**, 239 (1990).
[36] N. Nishi and K. Yamamoto, J. Amer. Chem. Soc. **109**, 7353 (1987).
[37] K. Yamamoto and N. Nishi, J. Amer. Chem. Soc. **112**, 549 (1990).
[38] K. Yamanaka, T. Yamaguchi, and H. Wakita, J. Chem. Phys. **101**, 9830 (1994).
[39] M. Ihara, T. Yamaguchi, H. Wakita, and T. Matsumoto, Adv. X-Ray Anal. Japan **25**, 49 (1994); T. Yamaguchi, H. Wakita, and K. Yamanaka, Fukuoka Univ. Sci. Reports **29**, 127 (1999).
[40] K. Furukawa, Rep. Progr. Phys. **25**, 395 (1962).
[41] J. Krogh-Moe, Acta Crystallogr. **2**, 951 (1956).
[42] N. Norman, Acta Crystallogr.**10**, 370 (1957).
[43] G. Johanson and M. Sandström, Chem. Scr. **4**, 195 (1973).
[44] T. Yamaguchi, Doctoral Thesis, Tokyo Institute of Technology, 1978.
[45] K. Ichikawa, Y. Kameda, T. Yamaguchi, H. Wakita, and M. Misawa, Mol. Phys. **73**, 79 (1991).
[46] A. H. Narten and H. A. Levy, J. Chem. Phys. **55**, 2263 (1971).
[47] A. H. Narten, J. Chem. Phys. **56**, 5681 (1972).